TECHNICAL MEMORANDUM

305

Salinity adjustments in the presence of temperature data assimilation

A.Troccoli, M. Balmaseda,
J. Segschneider, J. Vialard,
D.L.T. Anderson, K. Haines,
T.N. Stockdale and F. Vitart

Research Department

June 2000

European Centre for Medium-Range Weather Forecasts
Europäisches Zentrum für mittelfristige Wettervorhersage
Centre européen pour les prévisions météorologiques à moyen

Abstract

In this paper we evaluate the role of salinity in the framework of temperature data assimilation in a global ocean model that is used to initialise seasonal climate forecasts. It is shown that the univariate assimilation of temperature profiles, without attempting to correct salinity, can induce first order errors in the subsurface temperature field. A recently developed salinity scheme is used to improve the salinity field. In this scheme, salinity increments are derived from the observed temperature, by using the model temperature and salinity based on the T–S relationship preservation assumption.

Two data assimilation experiments were performed for the 9-year period 1990-1998. These show that the salinity scheme is effective at maintaining the halocline and thermocline structures especially in tropical regions. In addition to the improvement of the mean state, the scheme allows more temporal variability than relaxation to climatological data. Some limitations of the scheme are on occasion apparent, however. These limitations might be reduced in the future by use of altimeter sea level or sea surface salinity observations from satellite.

1 Introduction

A currently-used strategy to produce ocean analyses from which to begin seasonal forecasts is to force an ocean model with the recent history of windstress, heat fluxes and precipitation minus evaporation fields, and then use the analysed ocean state as initial conditions in a coupled ocean-atmosphere model. It is mainly the subsurface structure of the temperature fields which provides predictive skill on the time scale of a few months. The analysed ocean states are not perfect, however, as both forcing fields and ocean models contain errors. Ocean temperature data assimilation has proven to be capable of improving the simulated upper ocean temperature structure in such a way as to be beneficial for seasonal climate forecasting (e.g. Alves et al., 1999, Ji et al., 1998, Fischer et al., 1997, Rosati et al., 1997). The seasonal forecasting system at the European Centre for Medium-Range Weather Forecasts (ECMWF) uses an ocean analysis in which in situ temperature data have been assimilated.

Not much attention has been given to salinity in the context of temperature data assimilation for seasonal climate forecasts. Hitherto the most common approach has been to leave the salinity field unmodified when updating the temperature field. This is partly because subsurface salinity observations available in near real time are very sparse, and partly because the salinity field was thought to be of less importance for the density in the upper tropical ocean. However, as pointed out by Cooper over a decade ago (Cooper, 1988), salinity sometimes plays an important role in determining the three dimensional density structure even in tropical regions. More recently, salinity observations in the western equatorial Pacific revealed large interannual variations of salinity at subsurface levels

(Kessler, 1999, Ji et al., 2000). The physical causes for the observed anomalies are not fully explored yet, and it is therefore not clear to what extent the ocean analyses at ECMWF, in which salinity is treated as a prognostic tracer, can reproduce the observed changes.

Another, more technical issue, is that not modifying salinity when updating temperature may lead to generation of artificial and possibly unrealistic water masses which subsequently can corrupt the simulated ocean state. We will show that this can cause serious errors not only in salinity, but also in the temperature field.

Recently, several different attempts have been made to diagnose salinity even when temperature is the only subsurface data available. Some of the proposed methods make use of Empirical Orthogonal Functions (EOFs) to decompose the vertical structure of temperature (T) and salinity (S) profiles observed over limited regions and periods. The EOFs thus obtained are used to derive salinity when direct observations of S are not available. For example, Vossepoel et al. (1999) used 9000 T and S observations in the equatorial Pacific for the period 1975–96 (i.e. an average of about 3 observations in a 1° by 1° region per year), and Maes et al. (2000) used 778 profiles within the 10°S–10°N band along 165°E for the period 1984–1992 (these were all the profiles for which S was also measured). In the case of Vossepoel et al. (1999), the EOFs of the data provide a correction to their first guess which is obtained from a climatological T–S relation, so as to improve the S variability. Maes et al. (2000), on the other hand, utilise the EOFs as a first guess for reconstructing the salinity profiles (which might also be corrected towards a climatological value in case deviations become too large). In both cases, however, the representativeness of the EOFs depends on the availability of T and S observations. Because of the sparsity of S data, it is difficult to extend these results to regions outside the tropical Pacific. Further, the fact that EOFs can only represent structures that are present in the training data may prevent reconstructing S profiles that have not been observed in the past.

An approach that overcomes some of the limitations of the methods described above has been proposed by Troccoli and Haines (1999) (hereafter TH99). The basic idea is to use the T–S relationships of the closest, in time and space, T and S profiles to reconstruct the salinity profile from temperature information only. The approach has proven to be successful in the reconstruction of observed salinity profiles in the western tropical Pacific ocean when the T–S relationships are taken from observed profiles up to a few weeks before the time of the reconstruction (TH99). In the work presented here, observed T-S relationships are replaced by the T-S relationship of the model background, which is derived locally from the model T and S profiles. The main advantage of this approach compared to employing EOFs is that no learning period is needed. On the other hand, the scheme relies on realistic model T and S profiles. In order to test the method in a data assimilation framework, experiments have been devised using an ocean global circulation model, in which temperature data are assimilated.

The work is organised as follows. In section 2 the ocean model, the data assimilation system and the experiments are described. Results from the latter are presented in section 3. A discussion is provided in section 4.

2 Experimental set-up

This section presents the experimental set-up adopted in this work. The set-up chosen is slightly different from that used in the operational mode at ECMWF in that some parameters have been changed for this study. In particular, we use manually quality controlled data so guaranteeing that the same temperature data are used in both experiments. Further, the maximum depth to which data are assimilated is reduced from 1050 m to 425 m, to match the bottom of the TAO mooring observation profiles. Finally, a 3-day window is used in our experiments instead of a 10-day window in the operational set-up, thus giving more weight to the temperature observations in our experiments. In the following, a brief description of the ocean model is given first. Then the data assimilation system is described and, finally, the two experiments to test the TH99 salinity scheme are outlined.

2.1 Ocean model

The ocean model used in this work is the Hamburg Ocean Primitive Equation (HOPE) model (Wolff et al., 1997) modified by the Seasonal Forecast Project at the ECMWF and utilised for seasonal forecasting in coupled mode (e.g. Stockdale et al., 1998, Alves et al., 1999). Here we only describe its main features. It is a 3-D primitive equation model using z-coordinates and a variable sea surface height in a global domain. The model uses an E grid with a horizontal resolution of 2.8° x 2.8° (longitude/latitude), plus an equatorial refinement: the meridional resolution is 0.5° within 10° of the equator, and increases smoothly from 0.5° to 2.8° between 10 and 30 degrees. In the vertical there are 20 levels, 12 of which are in the upper 425 m. The parameterization of the vertical mixing uses a Richardson number dependent K-scheme, a modification of that of Pacanowski and Philander (1981). The K-value is increased mainly within the mixed layer, which is diagnosed as the depth-range in which temperatures differ by less than 0.5°C from the Sea Surface Temperature (SST). In order to avoid numerical problems with static instability, an *ad hoc* convection scheme is included, which mixes two adjacent model levels if $d\rho_\theta/dz > 0$ locally, where ρ_θ is the potential density.

The model is forced by daily average momentum, heat and fresh water fluxes taken from the ECMWF atmospheric analysis system. In order to avoid unrealistic drifts, additional weak restoring terms (time scale of 1 year) are applied to the 3-dimensional T and S fields by using annual climatological values from Levitus and Boyer (1994) and Levitus et al. (1994) (hereafter referred to as Levitus). An additional weak relaxation (time scale of 1 year) is applied to the Levitus surface S implying a damping time of 6 months for the surface salinity. A strong relaxation (time scale of 3 days) is applied to the surface temperature using weekly observational data (Reynolds and Smith, 1995).

2.2 Data assimilation system

The data assimilation method used in this study is an Optimal Interpolation (OI) derived from Smith et al. (1991). The observations utilised are sub-surface temperature mea-

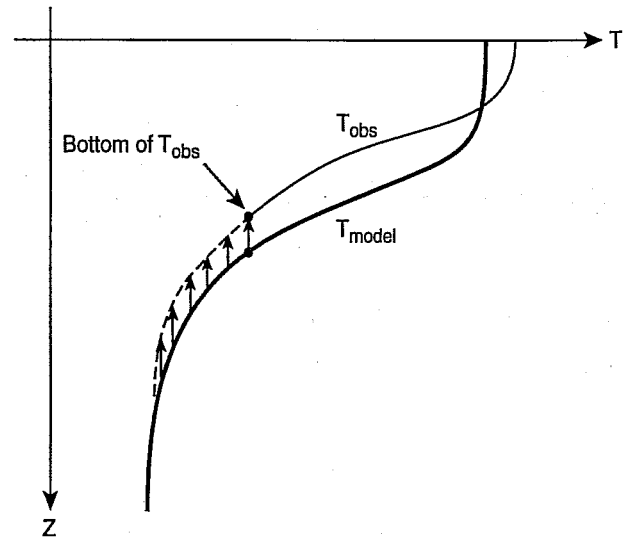

Figure 1: Schematic of the vertical displacement (first part of the TH99 scheme). The displacement is the difference between the depth of the deepest observed (or, as in our case, the output of the OI) temperature (thin solid line) and the depth of the same temperature in the model profile (bold solid line). This displacement is then used to lift (as in the figure) or lower the model profile in order to complete the observed profile below the deepest observed T (dashed line).

surements, obtained mainly from the United States National Oceanographic Data Center through the GTSPP (Global Temperature Salinity Pilot Project) data distribution network. The main components of the observing system are the XBTs and TAO moorings in the equatorial Pacific. TAO-type moorings in the tropical Atlantic from the developing Pirata array and PALACE float data distributed through the GTS are also used, even though these data types are much more recent and only impact towards the end of the experiments. The OI method is used to map these sub-surface temperature observations onto the model background. The observed T profiles are first interpolated onto the model levels, which are treated independently from each other in the OI. The OI of the temperature field (with the model T used as a background) is performed every 3 days, using observations grouped in 3-day bins in the TAO region and 10-day bins elsewhere. The data outside the TAO region are thus used more than once. Following Smith et al. (1991), the background is given the same weight as an individual observation. The background errors are expressed as anisotropic and inhomogeneous gaussian functions whose correlation length scales near the equator are 1500 km zonally and 200 km meridionally. In all the experiments described in this paper the assimilation is done over the levels from 2 to 12 (i.e. between 30 and 425 m depth). For further detail on the OI implementation in the HOPE model see Alves et al. (1999).

In order to obtain the updated vertical salinity profiles (i.e. the salinity analyses), the temperature profiles obtained by the OI are processed through an improved version of the TH99 scheme. This scheme is in two parts. First, a vertical displacement of the model background profile to match the bottom of the analysed T profile is made. The displacement corresponds to the difference between the depth of the deepest analysed

temperature and the depth of the same temperature in the model profile (an example is shown in Fig. 1). The salinity profile is also shifted by the same amount. This first part of the scheme reflects that isopycnal surfaces are often displaced even below the depth to which observations usually extend, e.g. by internal waves. The matching should help to prevent convective adjustments at the bottom of the observed profile. However, if the temperature at the bottom of the analysed profile is outside the T range of the model background, no displacement is performed. Typically, this may happen in coastal regions and at high latitudes. Second, the scheme computes an S analysis, using the T–S relationships from the model T and S background profiles. For example, at a T observation of 20°C, the analysed S will be the same as the S present at the depth of 20°C water in the model profile.

No information other than the temperature analysis (OI in the present case) and the model T and S profiles is needed for the TH99 scheme to work (see Fig. 2). It is known, however, that T–S preservation is not a good hypothesis when non-isentropic processes are dominating (e.g. in the mixed layer or in the vicinity of river inflow) for which T and S variations may be highly uncorrelated. Therefore, if the OI temperature is outside the range of the model T profile (as it may typically happen near the surface), then the model salinity is not modified. Also, in order to avoid applying the T–S relationships of near-surface water to deeper layers, the model T–S relationship from the upper 50 m of the water column is used only if the corresponding OI temperature is also near the surface. Otherwise, no change is made to the model salinity.

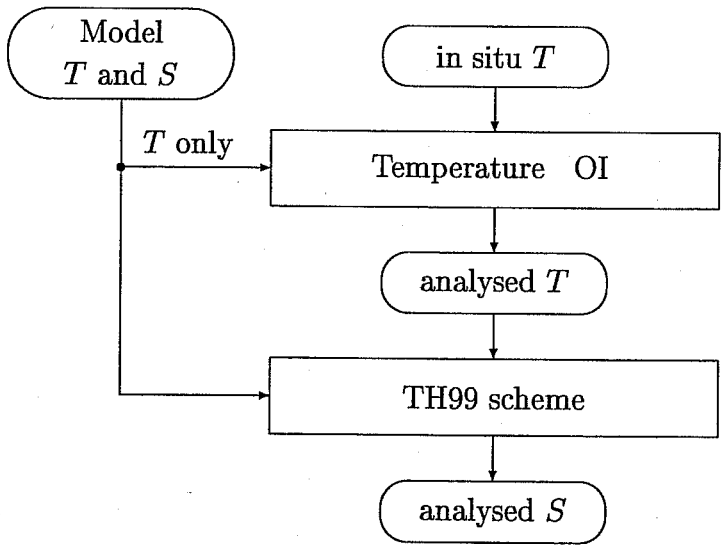

Figure 2: Schematic of the data assimilation system. TH99 scheme is the salinity scheme.

In addition, a latitudinal filter has been applied to the salinity increments such that the whole salinity increment is applied only within 30 degrees of the equator. Outside this region, the weight given to the salinity analysis diminishes linearly to zero at latitudes

poleward of 60 degrees. This is done to avoid implementing the TH99 scheme in areas where the stratification is weak and $S(z)$ persistence is more appropriate (see Emery and Dewar, 1982).

2.3 Description of the experiments

Three experiments, listed in Table 1, are run to test the TH99 salinity scheme. They all use the ocean model set-up described in section 2.1. The initial conditions are taken from a spin-up run which has been relaxed with a 10-day time scale to the Levitus climatology at all depths. The experiments are run for the period 1990 to 1998.

Experiment	Period (yr)	Assimilation
CNT	1990–1998	none
TOI	1990–1998	OI
TOIS	1990–1998	OI+TH99

Table 1: The three experiments. OI stands for Optimal Interpolation (temperature data only) and TH99 for the salinity scheme discussed in section 2.2.

To assess the impact of the TH99 salinity scheme on the OI analysis, two experiments are considered: one in which the TH99 salinity scheme is added to the OI (*TOIS*) and the other in which only the OI is used (*TOI*). In both experiments the temperature observations are presented to the OI procedure first. In *TOIS* the TH99 scheme is applied locally as a second step at each model grid point, as described in section 2.2. The T and S increments thus calculated are then uniformly added to the model background over a 3-day period, in order to allow the model to gradually adjust to the analysed density field. For reference, a run with no data assimilation is also performed (*CNT*), which will be mainly used to check how the data assimilation affects systematic model errors.

3 Assimilation results

In this section we analyse the impact of the TH99 salinity scheme, by comparing the two runs *TOIS* and *TOI* with observations (e.g. Levitus climatology) and the experiment *CNT*. We first analyse the 9-year mean in section 3.1 and then we investigate the salinity and the sea level variability in sections 3.2 and 3.3, respectively.

3.1 Analysis of the 9-year means

To investigate whether TH99 can improve the mean state, we examine time-averaged fields from the entire run (i.e. the 9-year mean 1990-1998). We first consider the equatorial

section through the Pacific and Atlantic oceans. The equatorial Pacific is an area relatively rich in T data and it is also a very important for seasonal forecasting.

Figure 3 and Figure 4 show temperature and salinity sections along the equator for the Pacific and Atlantic ocean. In each figure, panel (a) shows the climatological average from Levitus and panels (b-d) show the differences between *CNT*, *TOI*, *TOIS* and Levitus. Although we will use Levitus as a measure of climatology, it should be born in mind that it is not an absolute measure of the mean state of the oceans. For example the TAO thermal data have a somewhat different climatology in the west Pacific, either because of a different averaging period or a better data coverage during the TAO period. We will first discuss temperature. The dominant feature in Figure 3a is the sloping thermocline, which is an important feature of these two oceans. The *CNT* experiment shows substantial deviations of up to 3°C at the depth of the thermocline. The *CNT* experiment is warmer than Levitus in the eastern Pacific and in the Atlantic ocean, and colder in the western Pacific. The warmer temperatures in the Atlantic and eastern Pacific ocean are due to systematic bias in the *CNT* experiment. This bias is linked to a too diffuse thermocline in the model, possibly due to limitations of the mixing scheme combined with a poor vertical resolution. The assimilation of temperature profiles helps to control these errors. Figures 3c and 3d show that the errors are substantially reduced in *TOI* and *TOIS*, as a result of temperature assimilation. The differences between the assimilation experiments and Levitus in the western Pacific are likely to indicate differences between the Levitus and TAO climatologies. Levitus is based on data from 1900 to 1993 whereas the experiments span the 1990-1998 period. We compared the Levitus climatology with the TAO climatology from Yu and McPhaden (1999). and found that TAO was colder by about 2°C around 150 m depth in the western Pacific. Since the long-term mean of *CNT* is already consistent with the TAO data, the assimilation of temperature data does not change the thermal structure of *CNT* in the subsurface western Pacific very much.

Both the *TOI* and *TOIS* experiments improve the thermal state of the model at the thermocline level. Below the thermocline, however, significant differences with respect to Levitus, appear in *TOI* which is 1°C colder than Levitus around 300m and more than 2°C warmer than Levitus below 500 m in the Atlantic ocean. It is 1.2°C warmer than Levitus below 500 m in the eastern Pacific ocean. It must be noted that this corresponds to a vertical displacement of the isotherms on the order of 100 to 200 m at these depths. The differences between *TOI* and Levitus are thus quite large. These spurious differences are not present in *CNT* and must therefore be induced by the assimilation. They disappear in *TOIS* showing that the TH99 scheme helps to improve the deep ocean thermal structure in the assimilation. A discussion about the possible causes of the differences in the two experiments *TOI* and *TOIS* is deferred to later in this section, after introducing the salinity fields.

Figure 4 shows the salinity sections corresponding to the temperature sections from Figure 3. The Levitus climatology (Figure 4a) is characterized by relatively fresh water close to the surface, an intermediate salinity maximum around the depth of the thermocline, and monotonically decreasing salinity below. Low surface salinities are present at both the eastern and western boundaries in both oceans due to strong precipitation and/or river runoff. The subsurface salinity maximum is most pronounced in the western part

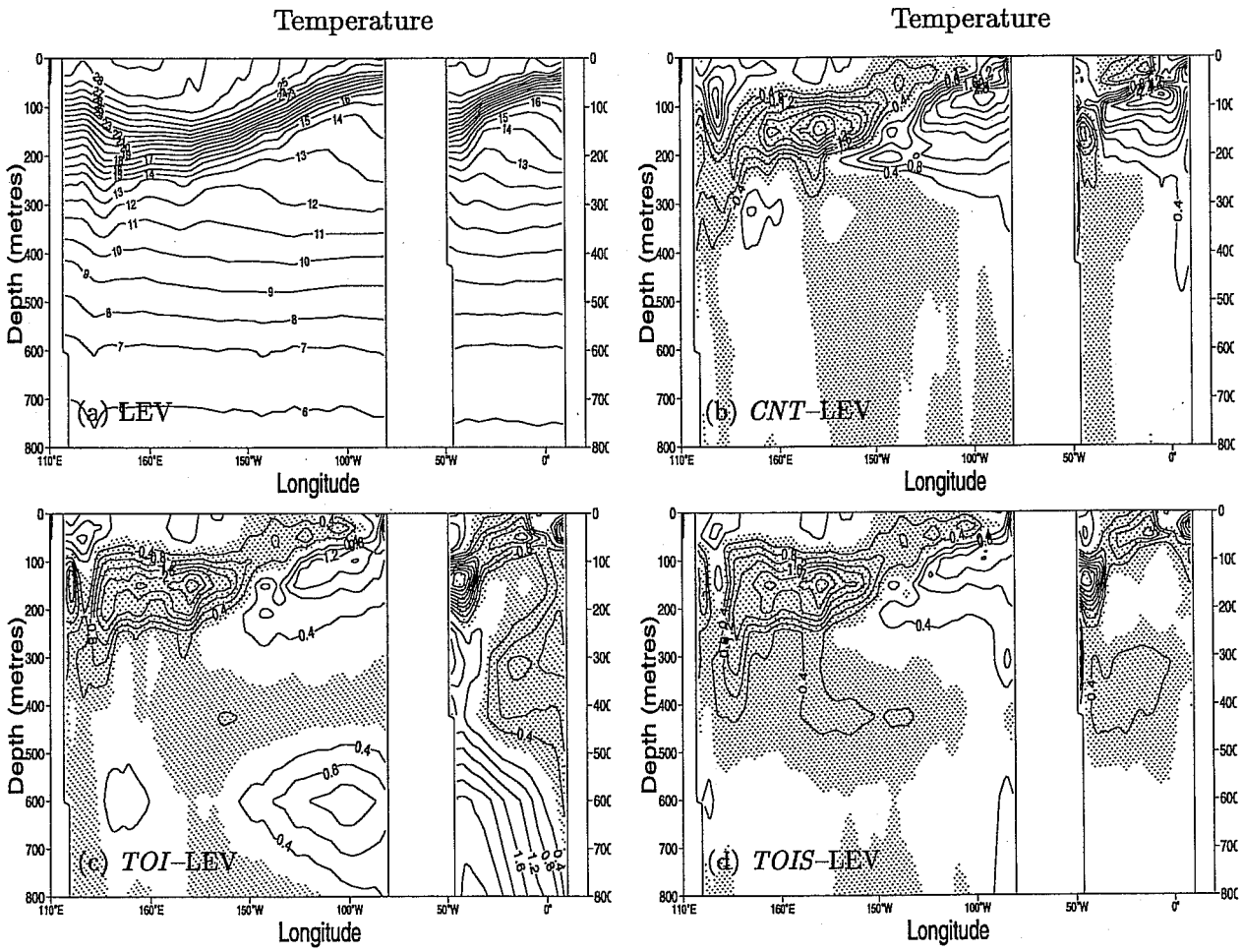

Figure 3: Equatorial sections of temperature. (a) Annual mean Levitus climatology; (b) the difference between the exp. *CNT* and Levitus averaged over the 9-year mean (1990-1998), (c) as for (b) but for the exp. *TOI* and (d) as for (c) but the exp. *TOIS*. Negative values are shaded.

of the basins. Because of errors in the specified surface freshwater flux and in the model formulation, *CNT* is different from Levitus (Figure 4b). It is fresher near the boundaries in the surface layer, and saltier around the subsurface salinity maximum. However, for the section shown, the departure from climatology is small below 200 m.

Figure 4c shows that the assimilation of temperature data in experiment *TOI* introduces large changes in the salinity field in the subsurface. In particular, salinity is lower than Levitus at around 200 m (by up to 0.8 psu in both the western Pacific and Atlantic). Below 300 m, salinity is higher than Levitus (by up to 0.2 psu in the Pacific and 0.6 psu in the western Atlantic). This indicates an export of salt from intermediate to deeper layers, as will be discussed later. The additional correction of salinity in experiment *TOIS* (Figure 4d) results in smaller differences with respect to Levitus salinity. The large differ-

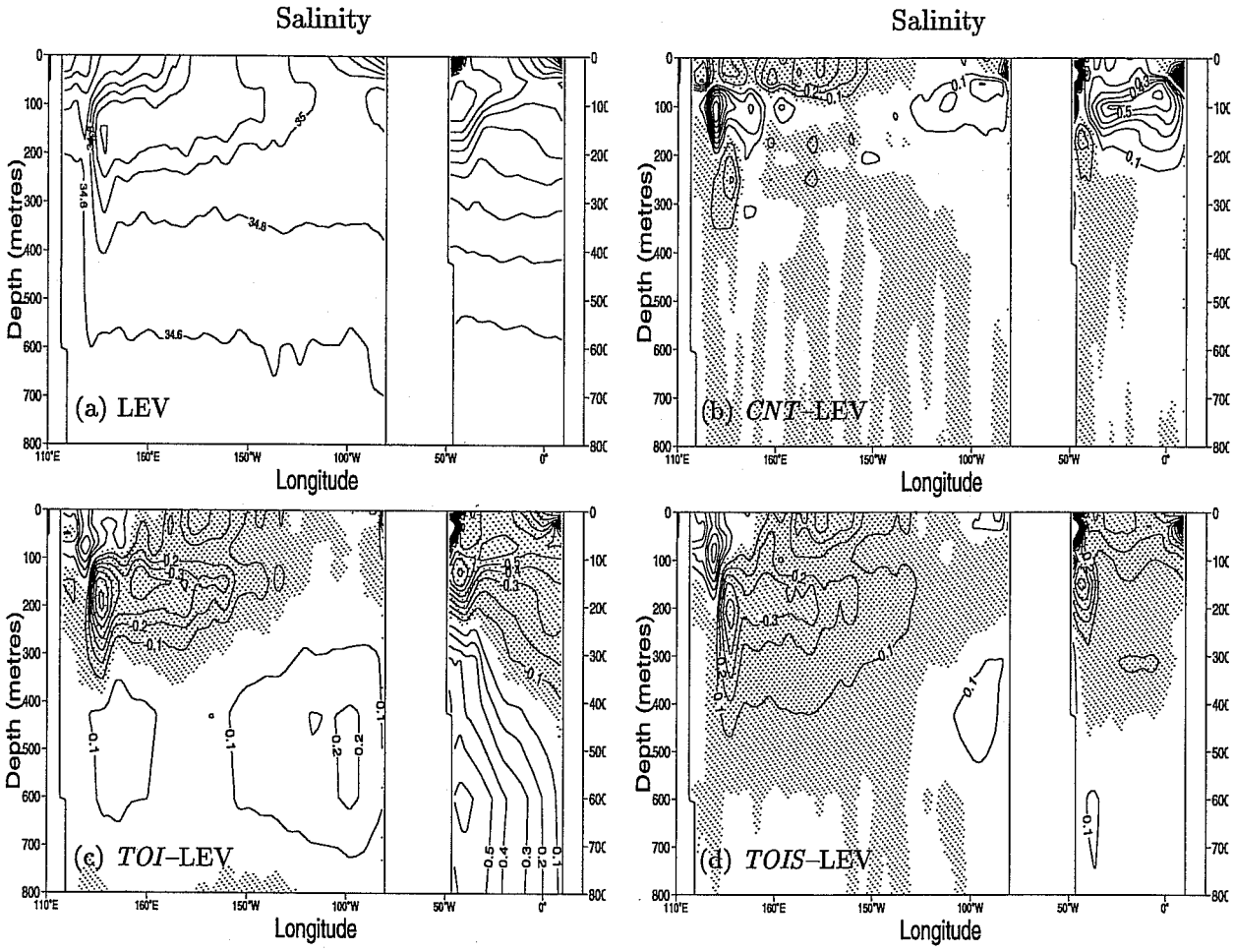

Figure 4: As in Fig. 3 but for salinity.

ences with Levitus that were present below 300 m in experiment *TOI* essentially disappear. At the thermocline level, they are significantly diminished in the Atlantic ocean. In the Pacific, the maximum deviations from Levitus are halved. All in all, below the depth of 50 m, *TOIS* shows a promising improvement over *TOI* when compared to Levitus. The behaviour of all three experiments is very consistent in the surface layer, but as mentioned earlier, we do not expect the TH99 scheme to improve surface layer salinity.

We can now start discussing possible causes of the differences between *TOI* and *TOIS*. Figure 5 shows meridional sections along 30°W of climatological temperature and of an instantaneous model output from *TOI*. After only three months, the temperature structure reveals large errors in the equatorial region. The isotherms between 5°N and 5°S have been displaced downwards in an unrealistic way in *TOI*. This is most likely caused by strong vertical mixing or convection in *TOI*. Very weakly stratified or unstable water columns can be created as the result of temperature assimilation in regions where there is a subsurface salinity maximum. Below this maximum, S decreases with depth and static stability is ensured by the temperature stratification. If the temperature increments given by the OI scheme in *TOI* are such as to decrease the vertical T stratification in these regions, (while S is left unchanged) the water column may become statically unstable. The model

mixing scheme then responds by spuriously increasing the vertical mixing. This is strongly reduced by the TH99 scheme in *TOIS*: the scheme adjusts the salinity profile in order to preserve T–S characteristics and thus mainly ensures static stability.

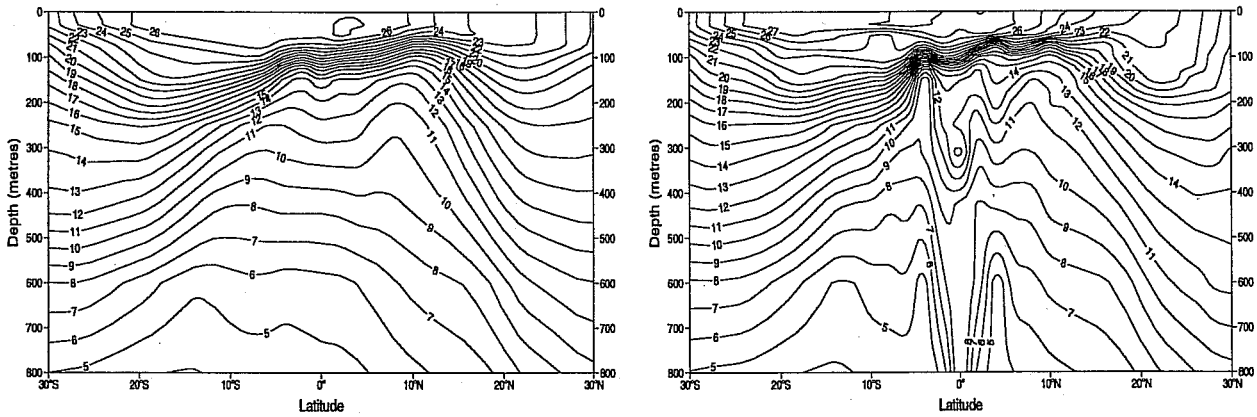

Figure 5: Meridional temperature section at 30°W. Left: initial conditions (i.e. climatology). Right: instantaneous field after a 3-month model integration with an Optimal Interpolation temperature assimilation (experiment *TOI*).

The spuriously increased mixing is most likely to occur where the salinity maximum in the main thermocline is relatively prominent or, more generally, when the salinity gradient below the S maximum is large. This explains why differences between *TOI* and *TOIS* are more pronounced in the equatorial Atlantic where the subsurface S maximum is stronger than in the Pacific.

An objective way of identifying those areas most likely to be affected by the enhanced mixing is provided by the following analysis. The stability of the water column can be expressed as the derivative of $\rho_\theta = \rho_\theta(\Theta, S)$ with respect to depth (z positive upward):

$$\frac{d\rho_\theta}{dz}(\Theta, S) = \left(\frac{\partial \rho_\theta}{\partial \Theta}\right)_S \frac{d\Theta}{dz} + \left(\frac{\partial \rho_\theta}{\partial S}\right)_\Theta \frac{dS}{dz} = -\alpha\, \rho_\theta \frac{d\Theta}{dz} + \beta\, \rho_\theta \frac{dS}{dz} \tag{1}$$

where ρ_θ is the potential density, θ the potential temperature α and β the thermal and haline expansion coefficients. In a statically stable water column $d\rho_\theta/dz$ is negative. In *TOI* the temperature profile is changed while the S profile is retained. If dS/dz is positive, this can lead to a statically unstable profile if temperatures are reduced at that depth by the OI. The critical value of the temperature stratification $(d\Theta/dz)_U$, which would cause convection to begin (when $d\rho_\theta/dz$ is zero) is given by:

$$\left(\frac{d\Theta}{dz}\right)_U = \frac{\beta}{\alpha}\frac{dS}{dz} = \gamma \frac{dS}{dz} \tag{2}$$

where $\gamma = \gamma(\Theta, S) > 0$.

If we assume, as shown by TH99, that temperature variability in the thermocline occurs mostly through vertical displacements of the water masses, it is possible to compute the minimum vertical displacement of the water column for which this will happen. The smaller this value, the greater the risk of spurious convection. Figure 6 shows the results of such evaluation with the temperature and salinity fields taken from the Levitus climatology along the equatorial section (left) and the 30°W meridional section (right). The solid lines show the minimum displacement, while the dashed line gives the depth at which instability occurs. The plot on the left shows that the Atlantic sector (between 50° W and 10° E) is more prone to instability than the Pacific sector. In the Atlantic, upward shifts of the temperature profile of between 15 m and 60 m (solid line) are generally sufficient to make the water column unstable at depths that vary between 90 m and 240 m (dashed line). In the Pacific these displacements are always more than 70 m and generally well over 100 m.

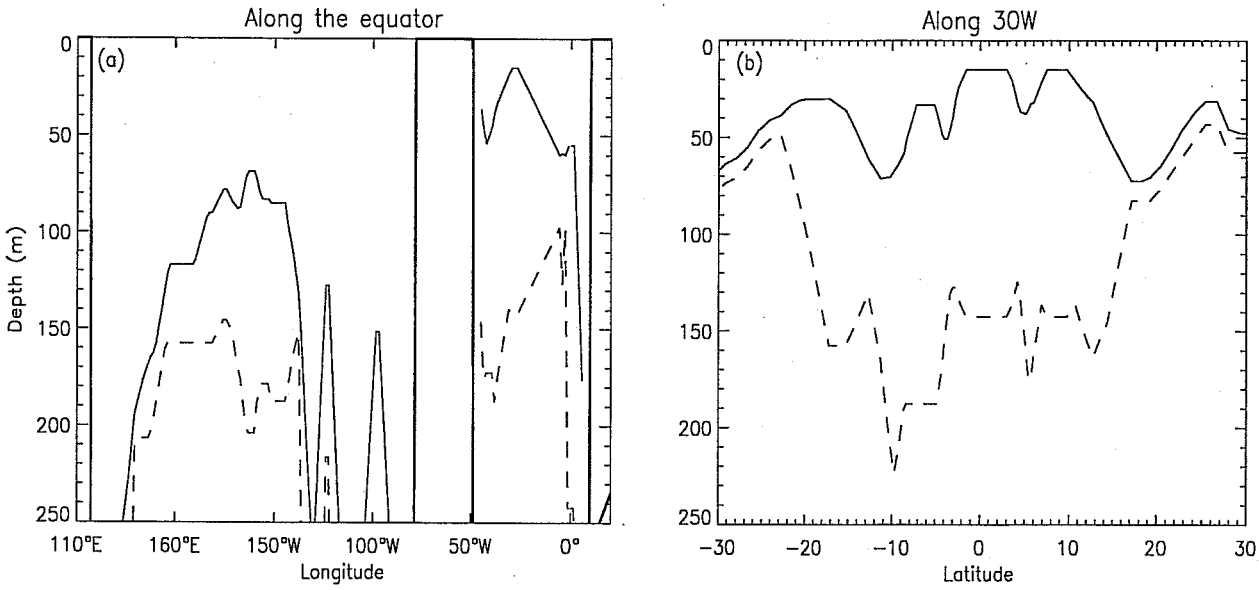

Figure 6: Minimum vertical displacement which would destabilise the water column (solid line) and depth of the corresponding level (dashed line). Along the equatorial section (a) and Atlantic meridional section at 30°W (b).

The above analysis yields a more rigorous confirmation of what could have been deduced from the climatological S in Fig. 4a: the S maximum in the Atlantic is up to 1 psu larger than in the Pacific, but the S values at depth are very close in the two oceans.

The smaller amount of temperature data collected in the Atlantic is another contributing factor as to why the T differences between *TOI* and *TOIS* are more pronounced in the equatorial Atlantic than in the Pacific, in particular in the thermocline. In the Atlantic during 1990-98 the main source of T profiles are XBT casts along shiptracks, so that observations at one location are only made a few times per year. Some of these will tend to generate spurious mixing and to erode both the temperature and salinity stratification. The only opposing effect to these damages to the T and S fields will be the relaxation to climatology which acts on the slow time scale of 1 year. On the other hand, in the Pacific ocean there are frequently repeated observations at the same location from the TAO array.

Once the salinity gradients have been eroded, the following temperature observations can constrain the temperature field without generating any spurious mixing or convection. The temperature field is thus very well constrained whereas the salinity field is still in error.

Note that in *TOI*, the assimilation makes no temperature increments below 425 m depth. This is an extreme "data sparsity" problem, and means that if the analysis starts to go wrong, there is nothing to bring it back other than the very slow relaxation to climatology. Thus, once a warm column begins to develop at these depths, it may be hard to stop. Extending the temperature analysis to lower depths might reduce this problem, or at least push it down deeper. In the experiments presented here, we chose 425 m instead of the operationally used 1050 m in order to match the depth to which TAO observations extend. It is mainly XBT observations that extend to greater depth. It might also be possible to formulate a bottom boundary condition of some sort to the temperature increments to help ensure stability. It is clear, however, that the present formulation of *TOI* has severe problems in maintaining the thermocline in the equatorial Atlantic.

To further study the impact of the TH99 scheme, we consider now a meridional section at the same location as for Figure 5 (30°W) but now for the nine year mean of the experiment. Figures 7a-d show the T and S fields for both *TOI* and *TOIS* and the difference between the two experiments (Figs. 7e-f). The T field is characterised by a tight thermocline between 8°S and 13 °N, whereas the S field presents two salinity maxima, and corresponding haloclines, one at about 17°S and the other at about 24°N. In Figs. 7a-b, starting at the base of the main thermocline, an anomalous warm and salty water column is seen in *TOI* in the neighbourhood of the equator. Such a feature is not present in the Levitus climatology: it is a manifestation of the spurious mixing activity discussed previously. On the other hand, the T and S fields of *TOIS* look more realistic (Figs. 7c-d), with only a slight bulge in the salinity field on the 34.6 psu isohaline near the equator and a corresponding though smaller bulge in the T field (5 and 6°C isotherms). This suggests that some strong mixing may still be occurring intermittently in the *TOIS* experiment, probably due to the fact that the assimilation does not take into account the actual depth of each observation profile (the deepest assimilation level is fixed, at 425 m). The difference between *TOI* and *TOIS* along this section (Figs. 7e-f) shows large discrepancies in T and S, especially in the 7°S - 8°N band, where the stability analysis (Fig. 6b) shows that instabilities are most likely.

We are now going to investigate the effect of the differences in T and S between *TOI* and *TOIS* on the density field. Fig. 8a shows an equatorial section of density and Figures 8b-c of temperature and salinity, respectively. In both oceans *TOI* is lighter than *TOIS* at the pycnocline level (around 150 m) and denser below. In the Pacific ocean, T differences between the two experiments are small (Fig. 8b). The density differences are thus mainly linked to the salinity (e.g. saltier water in *TOI* below the pycnocline results in denser water). In the Atlantic ocean, there is a competing effect of T and S on the density field (e.g. with *TOI* warmer and saltier below the thermocline). However, the salinity effect is once again dominating.

It is interesting to see the effect of these density differences between the two experiments in term of sea level. Because of the compensating effects of T and S differences, and because

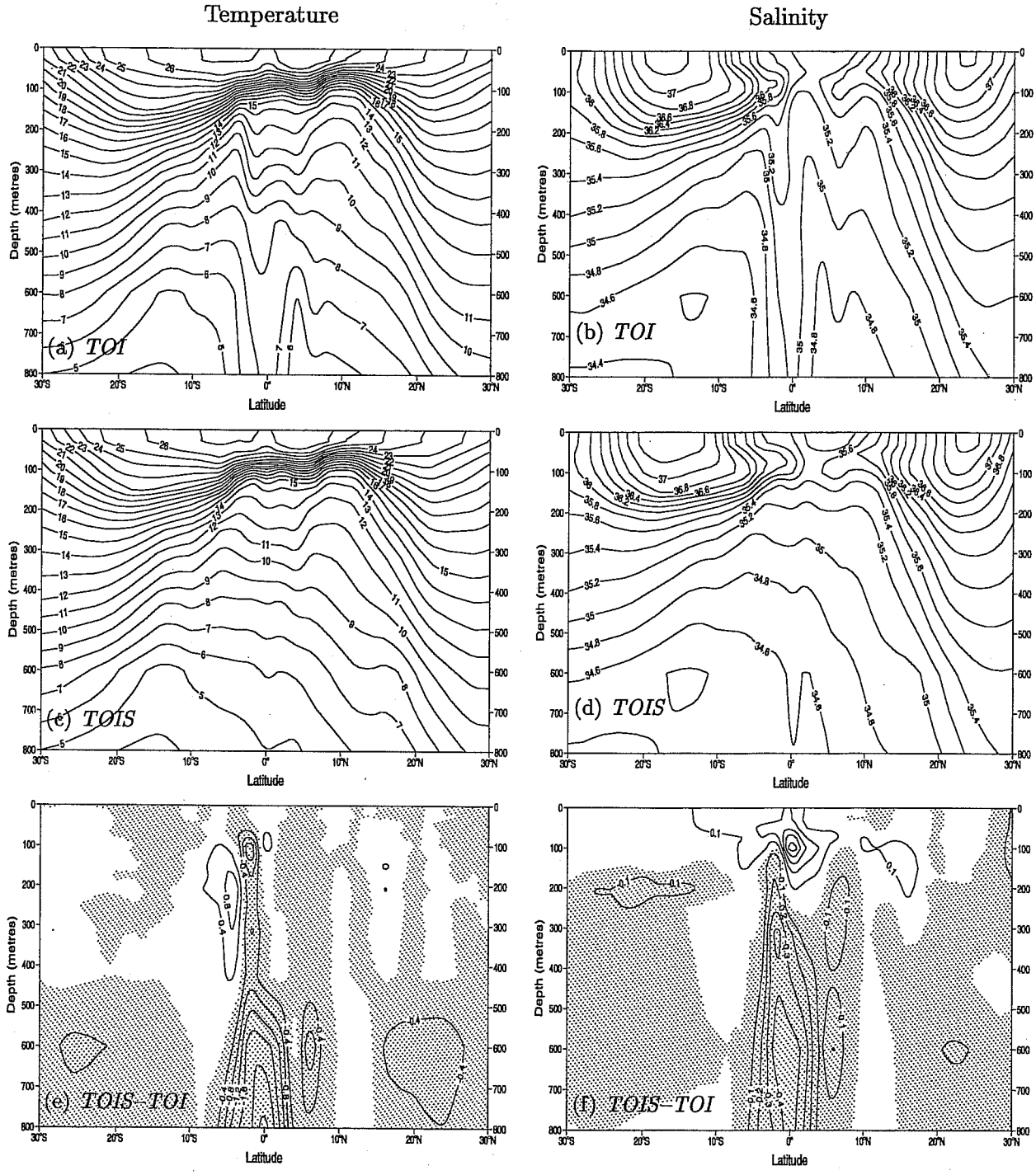

Figure 7: Meridional sections at 30°W of the 9-year mean (1990-1998). Temperature (a) and salinity (b) for the OI-only run (exp. *TOI*); Temperature (c) and salinity (d) for the OI plus salinity scheme run (exp. *TOIS*); *TOIS–TOI* temperature difference (e) and *TOIS–TOI* salinity difference (f). Negative values are shaded. The enhanced vertical mixing is evident in *TOI* between 7°S and 8°N (a-b). This causes large differences both in T and S between *TOIS* and *TOI* (e-f).

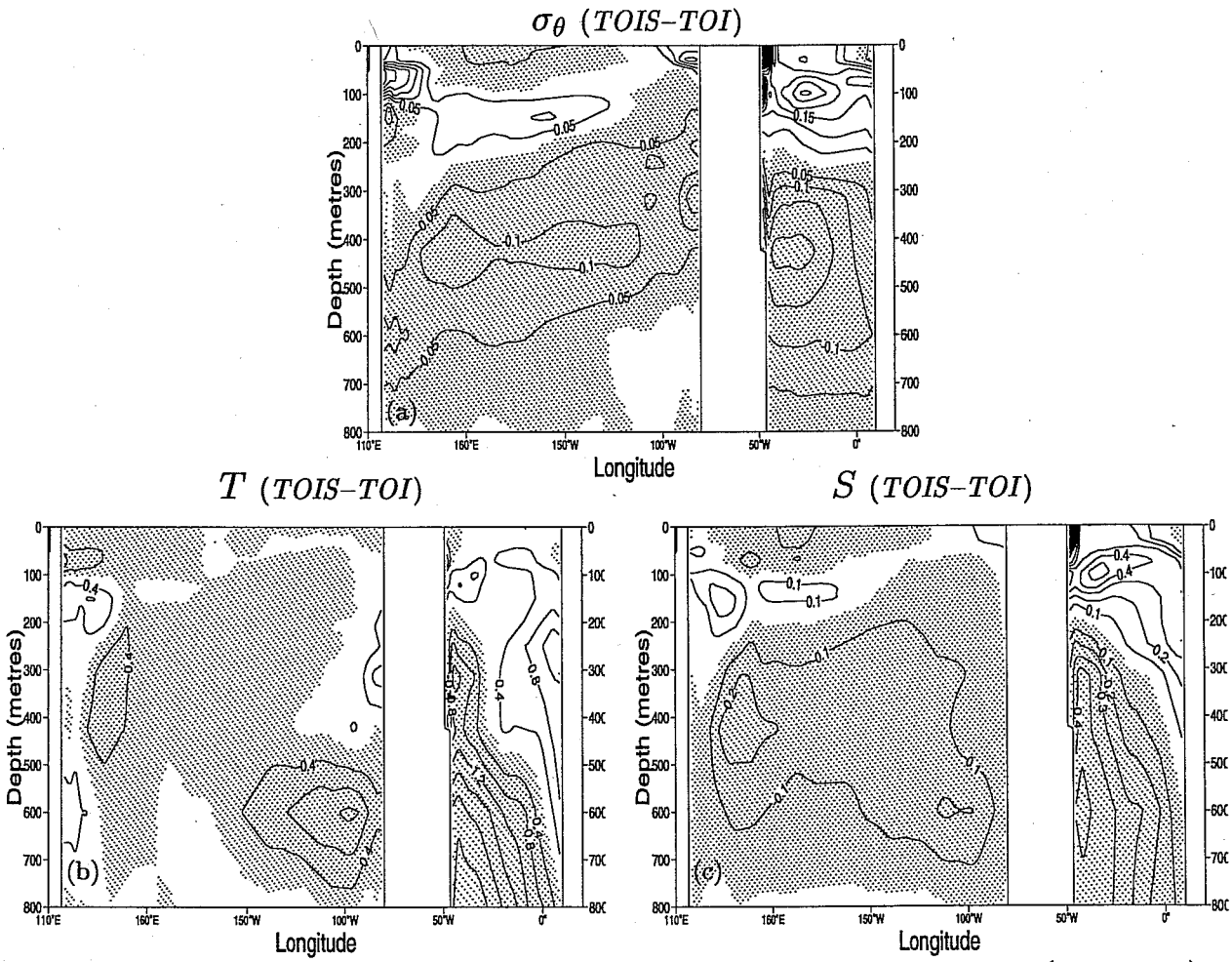

Figure 8: Equatorial section of the difference *TOIS–TOI* for the 9-year mean (1990-1998) for (a) σ_θ, (b) temperature and (c) salinity. Negative values are shaded.

of vertical compensation between denser water in *TOI* below the pycnocline and lighter water above, the overall difference in sea level is generally small. Along the equator in the Pacific and in the Atlantic, *TOIS* has a higher sea level than *TOI*, but the difference does not exceed 2 cm for the nine-year average (not shown).

3.2 Salinity variability

In the previous section we have shown that the use of the TH99 scheme generally improves the mean state of the ocean. However, for seasonal climate forecast initialization, the variability is also of concern. In this section we will examine how the TH99 scheme affects the salinity variability both by looking at differences between the time varying salinity fields in *TOI* and in *TOIS* and by comparing them with other modelling and observational results. Comparisons with CTD observations will also be made. In the next section we will compare the simulated sea level with Topex/Poseidon (T/P) sea level observations.

We focus attention on the tropical western Pacific ocean because subsurface salinity observations are relatively abundant in this region throughout the 1990–1998 period. The

section along 165°E is one of the best observed but even here data coverage is poor. The most thorough analysis of the temporal variability of salinity along the 165°E section is that of Kessler (1999) (hereafter K99). We will compare results from our model assimilations with K99's analysis, though direct comparison is not easy, since Kessler had to fill data gaps and smooth the results. Sometimes the section is occupied only twice in a year and then only at a couple of stations. Figure 1 from K99 illustrates this point very well.

Figure 9a shows the temporal evolution of the salinity maximum at 165°E, averaged over 3°S to 5°S for both *TOI* (dashed) and *TOIS* (solid). Kessler's interpolated values are shown by the heavy curve. We use the S maximum from the model and compare it with the equivalent observed quantity which has been recalculated for us by Kessler (priv. comm.), rather than the value of S on $\sigma_\theta = 24.5$ kg m^{-3} as in K99. The times of observations are shown by the crosses on the time axis. Only anomalies are plotted, relative to a mean spanning the years 1990-1996. The mean value salinity for K99 is 35.83 psu. The model mean values are all fresher than this. The difference is largest for *TOI*, 0.24 psu, somewhat smaller but still sizeable in the case of *TOIS*, 0.19 psu, and smallest in the case of the control, 0.11 psu. It should be noted, though, that these smaller values are partly due to the model vertical resolution which is much lower than that of CTDs.

With respect to the variability, the two assimilation experiments capture the low frequency signal seen in the data quite well, with high values in 1990–91, low values in 1992–93 and then increasing until 1996. This rising trend already discussed in K99 is not maintained after 1996 and salinity values drop in 1997. The extension of K99's analysis, to include later values after 1996 (priv. comm.), confirms the drop in salinity (Fig. 9a). Although the *TOI* values do not reach as low as those in *TOIS*, the drop from the peak in 1997 is just as large. The control integration *CNT* does not show such a large drop as either of the assimilation experiment and indeed agrees better with K99. We will return to this point later.

The model results all show more variability than the K99 curve, which is however a heavily smoothed interpretation of the data. It is difficult to say how appropriate the model variability is, but we note that both *TOI* and *TOIS* have larger fluctuations than *CNT*, and so there is a possibility that the data assimilation is introducing noise into the salinity field.

Still, it is not clear from this figure if *TOIS* is better than *TOI* or not. In Figure 9b, the anomalous depth of the salinity maximum is shown for the two experiments. The analysed depth from K99 is also shown, again heavily smoothed. This figure shows less obvious agreement between the model values and K99's analyses. What is obvious is that *TOI* has much wilder excursions than is the case for *TOIS*. These large excursions are related to the spurious mixing events in *TOI* discussed earlier. Although they are most acute at the equator, they can also occur off the equator as this figure shows. In terms of mean values, *TOIS* is closest to K99's data: 158 m for *TOIS* against 166 m for the latter. The mean values for *TOI* and *CNT* are 150 m and 144 m, respectively.

We now look at specific profiles and consider the event emphasised by Ji et al. (2000), for which salinity seems to play an important role in the density structure. Ji et al.'s two assimilation experiments, one with only T data and the other with T plus altimeter data,

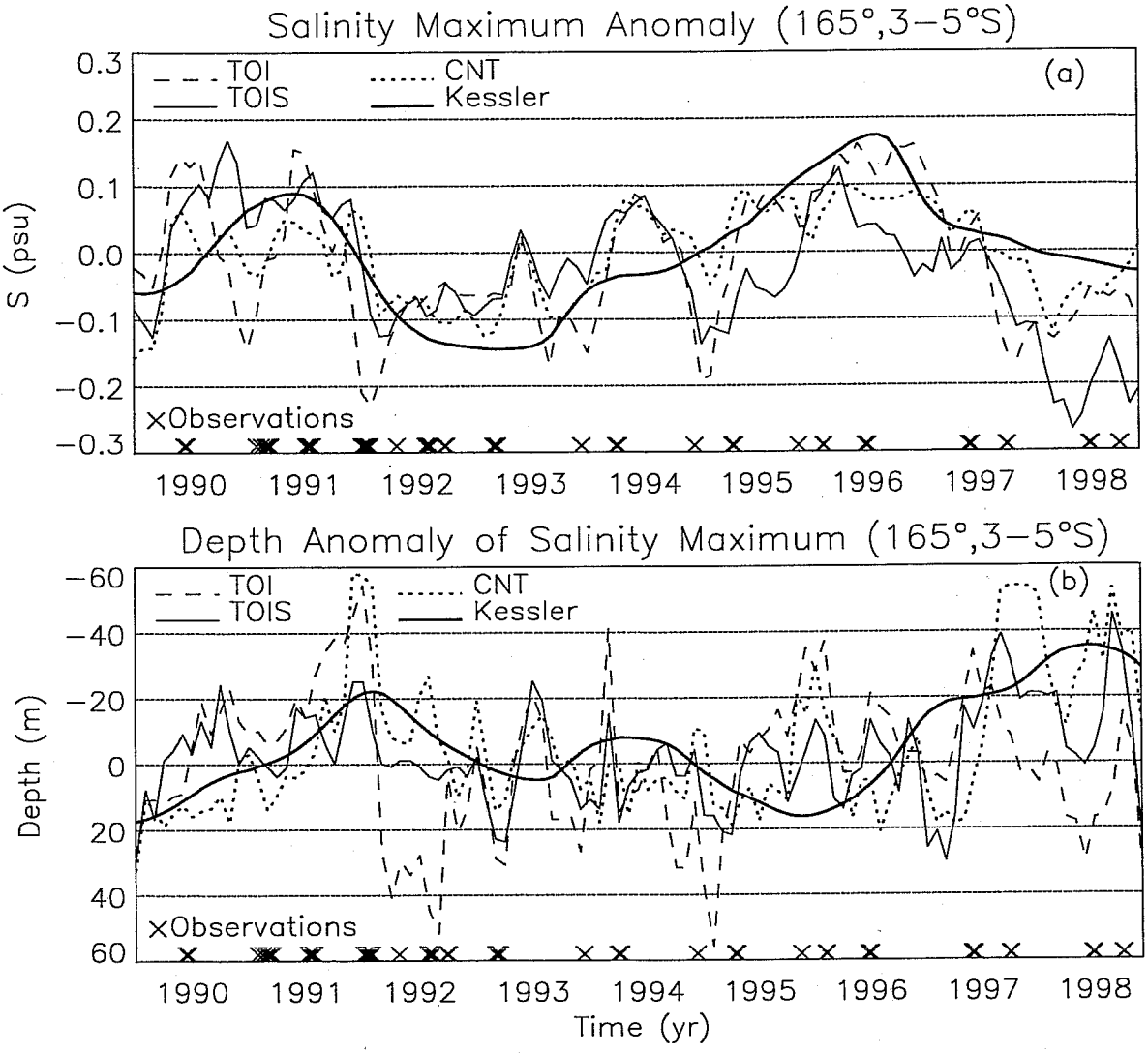

Figure 9: Temporal evolution at (165°E, 3-5°S) of the salinity maximum (a) and its depth (b) for *TOI* (dashed), *TOIS* (solid), *CNT* (dotted) and Kessler (1999) data (heavy line) with respect to their own 1990-1996 mean. The times of observations are shown by the crosses on the time axis.

yielded a large sea level difference (up to 9 cm), spanning several degrees of latitude around the equator between 140°E and 140°W, starting early in 1995 and peaking in mid-1996. In order to try to explain the cause of this sea level discrepancy, they examined the observed salinity difference taken from two CTD profiles at (165°E, 2°S), one at the beginning of the episode (2 May 1995, hereafter CTD95) and the other near its peak (10 July 1996, hereafter CTD96). In particular, the CTD95 salinity profile is fresher than the CTD96, down to a depth of about 180 m. Ji et al. argue that the interannual S variation would account for about 5 to 10 dyn cm difference comparable with the estimate of Maes and Behringer (2000).

In Figures 10a-b we consider the same two CTD profiles and compare them respectively with the May 1995 and July 1996 monthly average profiles for *TOI* and *TOIS*. These

comparisons will not be exactly equivalent because there is only one CTD profile available for each month at the chosen location, thus precluding a temporal average. [On a time scale of order one month, the CTD rms variability could be as large as 0.2 psu in the thermocline and even larger closer to the surface (Fig. 2 in TH99).] As a reference, the Levitus annual salinity profile at (165°E, 2°S), to which *TOI* and *TOIS* are relaxed, is also plotted in Figs. 10a-b.

The agreement of the S profile for May 1995 for *TOI* and *TOIS* with CTD95 is not particularly good (Fig. 10a). However, while the salinity maximum in *TOI* is marginally closer to CTD95, the shape of the profile in *TOIS* is more realistic both at the surface and at depth. As a consequence of the enhanced mixing, the S profile in *TOI* is almost homogeneous: S varies by only about 0.3 psu in the top 500 m, about half that of *TOIS*.

The observed salinity maximum in CTD96 of about 36 psu is not reached by either *TOI* or *TOIS* (Fig. 10b). However, *TOIS* agrees generally better than *TOI* with the observed profile, CTD96. In particular, the depth of the S maximum for *TOIS* is closer to that of CTD96. Both model profiles present a peculiar inversion at 250 m to 300 m depth. Since this is present in both *TOI* and *TOIS* we conclude that it is not a feature of the TH scheme. As it is not present in *CNT*, it must be caused by the OI procedure, and may be related to the fact that the T assimilation is done level by level.

Vossepoel and Behringer (2000) (hereafter VB) compare their model results with CTD casts also, using casts close to those shown in Fig 10. Ji et al. (2000) do not show model salinity profiles so we can not compare with their results. The fit to CTD96 in the top 250 m in Fig. 16 of VB is also poor, and worse than in *TOIS* by up to 50%: near the surface the difference with CTD96 is 0.25 psu compared to 0.17 psu in *TOIS*, and at the depth of the S maximum it is 0.75 psu compared to 0.5 psu in *TOIS*. Yet, below 250 m the fit to CTD96 in VB is very good, better than in either of our assimilation runs or in our control run. This may arise in part from the time scale used to relax the salinity to climatology: we have a relaxation constant of 1 year, whereas they use a value of 50 days. However, it is generally not easy to compare the results of two assimilation methods. The VB method is active only in the upper hundred meters or so. In our approach, there is no such restriction.

Whilst one would expect a better fit at depth (as in Fig. 16 of VB, or indeed between Levitus and CTD96 in Fig 10b), it should also be noted that some salinity variability is still present even below 250 m. For example, Fig. 2 in Vossepoel et al. (1999) shows a standard deviation of 0.1 psu at around 300 m, even though a much more local analysis yielded a value of 0.02 psu (Fig. 2 in TH99). In any case, this salinity variability indicates that a strong feedback to climatology is not necessarily desirable.

The salinity variability is further analysed by means of a Hovmoller plot of $S(z)$ at (165°E, 2°S) for *TOI* (Fig. 11a) and *TOIS* (Fig. 11b). The episodic and extended flooding of the deeper layers with high salinity water (more than 35 psu, i.e. unshaded regions) is clearly visible in *TOI*, as for instance in the 1993-95 period. This is the effect of the strong vertical mixing discussed in section 3.1 and it does not appear in *TOIS* (Fig. 11b).

The interannual S variability in the *TOIS* run looks generally plausible. Several features of the variability seem to correspond with K99's data from Figure 9, although the location

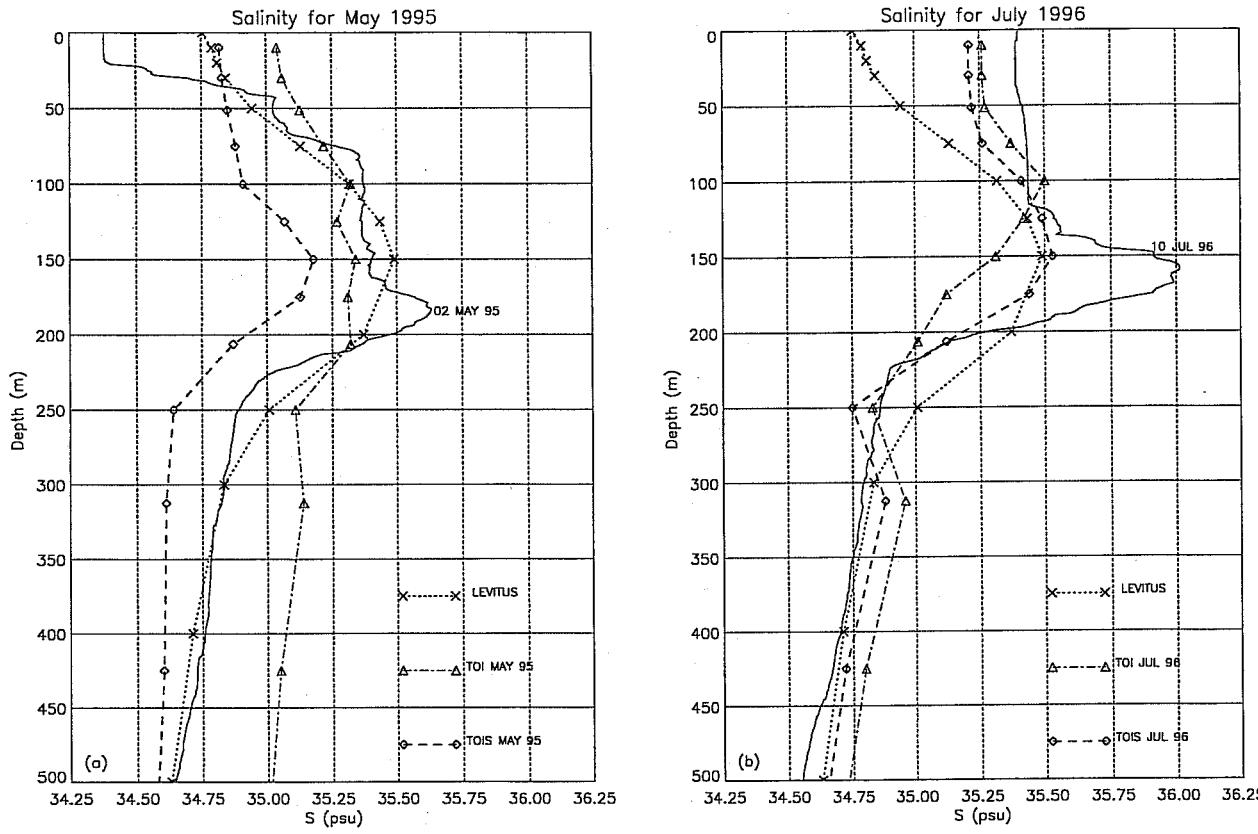

Figure 10: Salinity profiles at (165°E, 2°S) from instantaneous CTD data (solid lines) and monthly averages for *TOI* (dash-dotted) and *TOIS* (dashed) for May 1995 (a) and July 1996 (b). Also plotted is the annual Levitus salinity profile (dotted) to which *TOI* and *TOIS* are relaxed.

of the data is slightly further south than the area plotted here. Note that the persistent salinity maximum (S larger than 35.4 psu), from the beginning of 1990 to the second half of 1991, as well as the salinity up-lifting, corresponding to the 1991-1992 El-Niño, are in agreement with the observations. Also, the shoaling of the S maximum associated with the 1994-1995 warm event and the increase in the salinity maximum starting at the beginning of 1996 are represented by *TOIS*. Figure 11 also shows the dates on which the two profiles of Figure 10 were taken. Because of the relatively high frequency variability in both model assimilations, it is clear that comparing individual profiles can give only limited information on how well interannual variability is represented. This fact, coupled with the sparsity of the observed data and thus our inability to produce plots such as Figure 11 from data, means that a detailed and reliable assessment of *TOI* and *TOIS* in terms of salinity variability is not possible. Clearly some broad features are captured, as shown in Figure 9, but salinity data does not (yet) have the space time coverage to say much more than this.

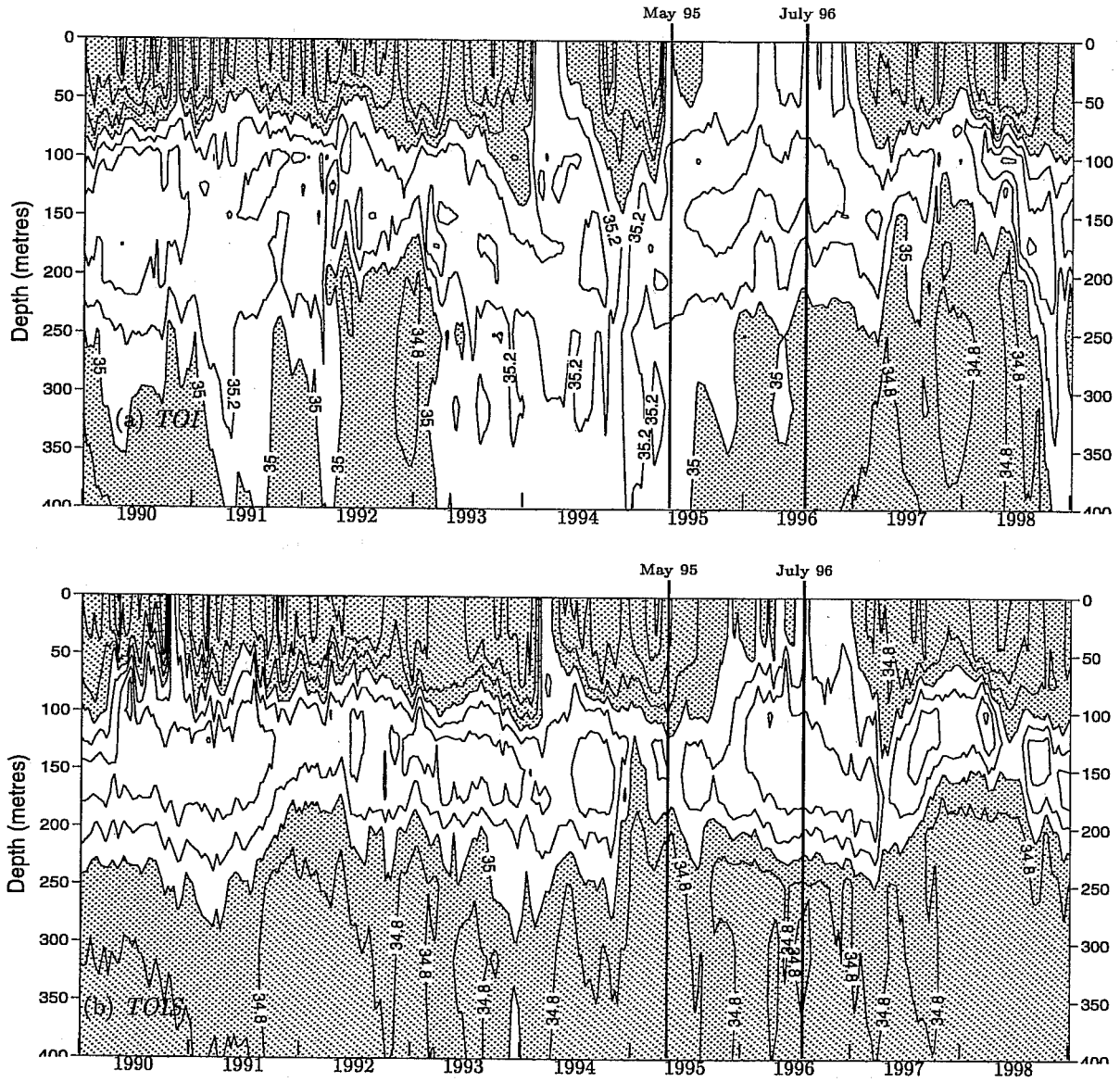

Figure 11: Salinity as a function of depth and time at (165°E, 2°S) for *TOI*(a) and for *TOIS* (b). Shading for values smaller than 35 psu. Contour interval is 0.2 psu.

3.3 Sea level variability

We will now assess the impact of the TH99 scheme on the sea level variability. We begin by considering the 1995–96 period. Ji et al.'s temperature data assimilation experiment showed poor representation of sea level in the case when only T was assimilated and this lead them to examine the role of salinity. Our corresponding experiment, *TOI*, does not show this disagreement when compared to T/P altimeter data. This does not mean that we recreate the subsurface salinity well but the convective readjustments present in *TOI* lead to little or no changes in sea level. In particular, in terms of sea level, both *TOI* and

TOIS are able to reproduce this particular event rather well: differences between *TOI* and *TOIS*, as well as between each of them and altimeter data, are within 2–3 cm, for this region (after removing the 1993-1995 mean in each case).

In Figures 12a-d we show the comparison between the T/P sea level observations and *TOIS* (a and c) and *TOI* (b and d) in terms of rms errors (a-b) and correlations (c-d) for the period 1993-1998. These plots have been constructed by taking the T/P gridded products (Le Traon et al., 1998) and the corresponding model fields.

Along the equator in the Pacific, the agreement between the two assimilation experiments and the sea level observations (i.e. T/P) is good. Rms errors with respect to T/P are about 3-4 cm for both *TOIS* and *TOI* (Figs. 12a-b), with *TOI* marginally better than *TOIS*. One region where the rms-error differences are larger than the 2–3 cm rms error in T/P is located in the central Pacific at (140°W, 8°S, Fig. 12a). What gives rise to this difference has yet to be determined but we know it is a problem in *TOIS* since the rms difference between *TOI* and T/P shows no anomalous behaviour there whereas *TOIS* shows large errors (cf. Figs. 12a-b). This is further confirmed by Figure 13 which shows the rms differences between *TOI* and *TOIS*.

Rms errors in the equatorial Atlantic are generally larger than in the equatorial Pacific. The better performance of the Pacific over the Atlantic is mainly caused, as noted in section 2.2, by the larger amount of temperature data available for assimilation in the Pacific. In the Atlantic, T observations are more sporadic since they derive from the XBT network rather than the TAO-type array in the Pacific which reports daily.

The correlations between T/P and model sea level (Figs. 12c-d) basically confirm the results supplied by the rms errors. In the equatorial Pacific, the correlation is larger than 90% for both *TOIS* and *TOI*. In the equatorial Atlantic, the correlation is less encouraging as it exceeds 70% only in a limited domain.

It should be pointed out that in the rms errors and correlations thus far presented the seasonal cycle is included. We also removed the seasonal cycle, so as to analyse the interannual variability (figures not shown), and diagnosed three different behaviours for the Pacific, Atlantic and Indian Ocean. In the Pacific the assimilation experiments (*TOI* and *TOIS*) have a better fit with T/P than experiment *CNT*. In the Atlantic, instead, the opposite is true, i.e. *CNT* is better than both *TOI* and *TOIS*. Lastly, in the Indian ocean all three experiments are roughly equivalent. These diverse behaviours can be explained by the different amount of temperature observations available for assimilation. In the case of the Pacific, the amount of data is such as to constrain well the interannual variability, whereas the sporadic availability of measurements in the Atlantic affects the variability in such a way as to worsen the interannual variability. Finally, in the Indian ocean where the T observations are even less abundant than in the Atlantic, the impact of the data assimilation is nearly negligible.

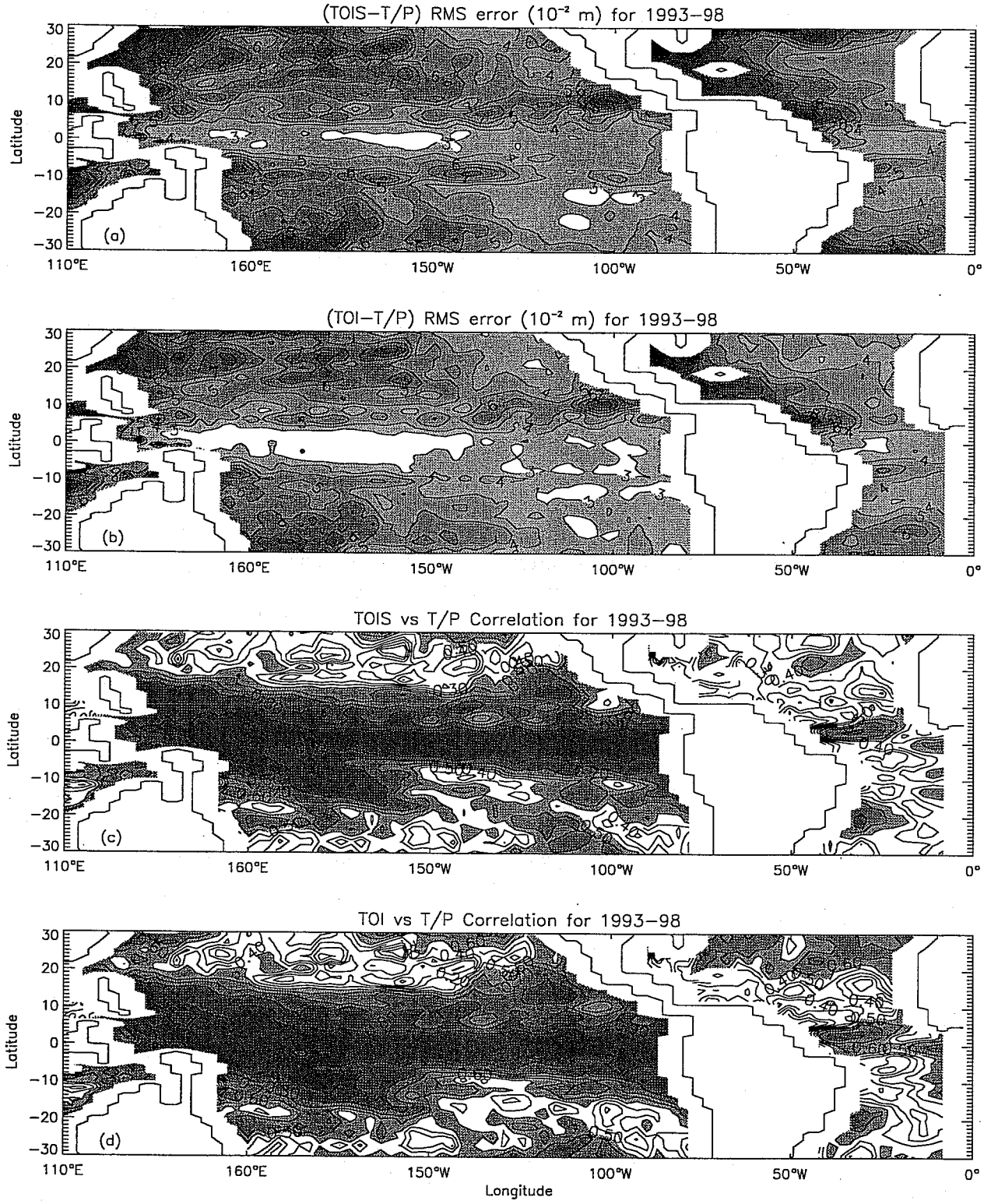

Figure 12: Sea surface height rms errors (a-b) and correlations (c-d) for *TOIS* and *TOI* with respect to TOPEX/Poseidon for the period 1993-98. In (a-b) contour interval is 1 cm and shading for values greater than 3 cm; in (c-d) contour interval is 0.1 (10%) and shading for values greater than 0.5 (50%). Data are masked in the vicinity of land points.

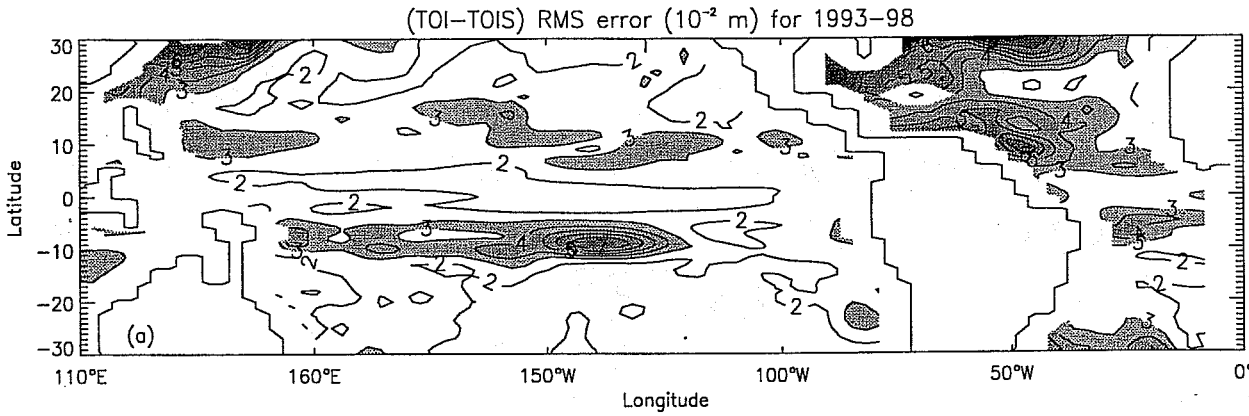

Figure 13: As in Figs. 12a-b but for *TOI* with respect to *TOI*.

4 Discussion

The salinity scheme proposed by Troccoli and Haines (1999) has been applied to the ocean model used at ECMWF, by combining it with the pre-existing temperature Optimal Interpolation (OI) procedure. An experiment in which salinity was corrected (*TOIS*) has been run for the 1990–1998 period and was compared with one in which only temperature is updated (*TOI*). The 9-year mean analysis has shown promising results for *TOIS*, with significant salinity improvements, with respect to *TOI*, especially below 50 m depth. Indeed, persisting $S(z)$ in regions where salinity decreases with depth can lead to first-order error in the model mean state. The water column can become statically unstable and lead to spurious vertical mixing when the temperature increment tends to decrease the thermal stratification. This has a particularly dramatic effect in the tropical Atlantic where there is a strong salinity maximum and where there are not many data to constrain the temperature field. In the experiment *TOIS*, these first-order errors are virtually eliminated as the TH99 scheme allows preservation of water mass properties, thus preventing spurious convection from occurring.

In spite of the fact that the salinity profile is generally better reproduced by *TOIS* than *TOI*, the sea level variability, measured by the rms errors between the T/P sea surface height and the two model experiments, is not noticeably improved with *TOIS*. In fact, rms errors and correlations are slightly better in *TOI*, when referred to an independent data set such as T/P sea level.

The approach of this paper has been to use in situ thermal data to correct salinity. An EOF-based similar type of approach has also been tested by Maes (1999) and Vossepoel et al. (1999), but in their schemes an extensive back history of salinity is needed both in space and time in order to derive the EOFs. This is a serious limitation in applying the scheme in a global assimilation system such as that used at ECMWF. Indeed, one of the regions of improved response of our scheme was shown to be the Atlantic where the mean state was substantially improved. The Atlantic, an area with limited T and S data coverage, was not considered by either Maes (1999) or Vossepoel et al. (1999).

We have shown that the TH99 scheme has its limitations. Both Vossepoel and Behringer (2000) and Maes and Behringer (2000), have extended their schemes to include altimetry. This is clearly a next step for us too. The use of altimeter data in the ECMWF system has been explored with encouraging results by Segschneider et al. (2000). We have not yet combined the scheme described here with altimeter data from T/P but work is in progress. One of the main reasons for us becoming interested in salinity came from comparing the model sea-level with real-time altimeter data as part of the DUACS programme of the European Community. This lead to a realisation that salinity was being handled badly in our real-time analysis system. Therefore, we believe that adding the altimeter information to the system presented in this work can only improve the performance of our simulations.

Both Vossepoel and Behringer (2000) and Maes and Behringer (2000) have considered using surface salinity. A better representation of the sea surface salinity (SSS) would greatly improve the top 50 m of the vertical salinity profile, as found by Reynolds et al. (1998). The SSS signal is unable to penetrate below this depth, but combining surface salinity measurements with the TH99 scheme should provide a better analysis throughout the water column. This is not idle speculation as there is a real prospect that SSS observations from satellite will become available in the not-too-distant future (Lagerloef et al., 1995), which would thus render this solution possible.

All in all, our results show a method which can overcome many of the troublesome aspects of a univariate OI scheme. It is not, however, a panacea. The concept of T–S conservation is inappropriate in the surface layer, but the TH99 method does seem to work moderately well beneath this layer. Hence, SSS data would greatly help to improve the assimilation scheme. In fact, whilst we could obtain some improvement in the salinity analysis either by including altimeter data or improving the assimilation scheme, it seems unlikely that the salinity field will be well reproduced in ocean models without the inclusion of salinity observations, not only at the surface but also from the subsurface.

Acknowledgements

Part of this work has been supported by the European Union Environment and Climate project DUACS (ENV4-CT96-0357). The altimeter products have been produced by the CLS Space Oceanography Division as part of the European Union Environment and Climate project AGORA (ENV4-CT9560113) and DUACS (ENV4-CT96-0357). Author AT received support from the NERC through a WOCE grant during the early part of this work. We thank Jocelyn Williams for drawing Figure 1 and Michael McPhaden for supplying us with the CTD data used in Fig. 10 and Billy Kessler for the data used in Figure 9, including extending his analysis to the end of 1998 for us.

References

Alves, J. O. S., Anderson, D. L. T., Stockdale, T. N., Balmaseda, M. A. and Segschneider, J.: 1999, Sensitivity of ENSO forecasts to ocean initial conditions, *Proceedings of the*

International Symposium, Triangle'98, Sep 29-Oct 2, Kyoto, Japan, pp. 21–30.

Cooper, N.: 1988, The effect of salinity on tropical ocean models, *J. Phys. Oceanogr.* **18**, 697–707.

Emery, W. J. and Dewar, L. J.: 1982, Mean temperature-salinity, salinity-depth and temperature-depth curves in the North Atlantic and North Pacific, *Prog. in Oceanography* **16**, 219–305.

Fischer, M., Latif, M., Flugel, M. and Ji, M.: 1997, The impact of data assimilation on ENSO simulations and predictions, *Mon. Wea. Rev.* **125**, 819–829.

Ji, M., Behringer, D. W. and Leetmaa, A.: 1998, An improved coupled model for ENSO prediction and implications for ocean initialization. Part II: The coupled model, *Mon. Wea. Rev.* **126**, 1022–1034.

Ji, M., Reynolds, R. W. and Behringer, D. W.: 2000, Use of TOPEX/Poseidon sea level data for ocean analyses and ENSO prediction: Some early results, *Journal of Climate* **13**, 216–231.

Kessler, W. S.: 1999, Interannual variability of the subsurface high salinity tongue south of the Equator at 165°E, *J. Phys. Oceanogr.* **29**, 2038–2049.

Lagerloef, G. S. E., Swift, C. T. and Vine, D. M. L.: 1995, Sea surface salinity: the next remote sensing challenge, *Oceanography* **8**, 44–50.

Le Traon, P. Y., Nadal, F. and Ducet, N.: 1998, An improved mapping method of multi-satellite altimeter data, *J. Atmos. Oceanic Technol.* **15**, 522–534.

Levitus, S. and Boyer, T. P.: 1994, World Ocean atlas 1994. Volume 4: Temperature, *Technical Report No. 4*, U.S. Department of Commerce, National Oceanographic and Atmospheric Administration. 129 pp.

Levitus, S., Burgett, R. and Boyer, T. P.: 1994, World Ocean atlas 1994. Volume 3: Salinity, *Technical Report No. 3*, U.S. Department of Commerce, National Oceanographic and Atmospheric Administration. 111 pp.

Maes, C.: 1999, A note on the vertical scales of temperature and salinity and their signature in dynamic height in the western Pacific Ocean: Implications for data assimilation, *J. Geophys. Res.* **104**, 11 037–11 048.

Maes, C. and Behringer, D. W.: 2000, Using satellite-derived sea level and temperature profiles for determining the salinity variability: a new approach, *J. Geophys. Res.* submitted.

Maes, C., Behringer, D. W., Reynolds, R. W. and Ji, M.: 2000, Retrospective analysis of the salinity variability in the western tropical Pacific ocean using an indirect minimization approach, *J. Atmos. Oceanic Technol.* in press.

Pacanowski, R. C. and Philander, S. G. H.: 1981, Parameterization of vertical mixing in numerical models of the tropical oceans, *J. Phys. Oceanogr.* **11**, 1443–1451.

Reynolds, R. W. and Smith, T. M.: 1995, A high resolution global sea surface temperature climatology, *Journal of Climate* **8**, 1571–1583.

Reynolds, R. W., Ji, M. and Leetmaa, A.: 1998, Use of salinity to improve ocean modeling, *Phys. Chem. Earth* **23**, 543–543.

Rosati, A., Miyakoda, K. and Gudgel, R.: 1997, The impact of ocean initial conditions on ENSO forecasting with a coupled model, *Mon. Wea. Rev.* **125**, 754–772.

Segschneider, J., Anderson, D. and Stockdale, T.: 2000, Towards the use of altimetry for operational seasonal forecasting, *Journal of Climate.* in press.

Smith, N. R., Blomley, J. E. and Meyers, G.: 1991, A univariate statistical interpolation scheme for subsurface thermal analyses in the tropical oceans, *Prog. in Oceanography* **28**, 219–256.

Stockdale, T. N., Anderson, D. L. T., Alves, J. O. S. and Balmaseda, M. A.: 1998, Global seasonal rainfall forecasts using a coupled ocean-atmosphere model, *Nature* **392**, 370–373.

Troccoli, A. and Haines, K.: 1999, Use of the Temperature-Salinity relation in a data assimilation context, *J. Atmos. Oceanic Technol.* **16**, 2011–2025.

Vossepoel, F. C. and Behringer, D. W.: 2000, Impact of sea level assimilation on salinity variability in the western equatorial Pacific, *J. Phys. Oceanogr.* in press.

Vossepoel, F. C., Reynolds, R. W. and Miller, L.: 1999, Use of sea level observations to estimate salinity variability in the tropical Pacific, *J. Atmos. Oceanic Technol.* **16**, 1401–1415.

Wolff, J., Maier-Reimer, E. and Legutke, S.: 1997, The Hamburg Ocean Primitive Equation model, *Technical Report No. 13*, Deutsches KlimaRechenZentrum, Hamburg.

Yu, X. and McPhaden, M.: 1999, Seasonal variability in the equatorial Pacific, *J. Phys. Oceanogr.* **29**, 925–947.